Supplementary materials and methods

Sphere formation assay

To assay sphere formation efficiency, a single-cell suspension of HCC cells was created in serum-free DMEM/F12 medium (cat# 12400-024; GIBCO) with 20 ng/ml human recombinant epidermal growth factor (EGF; cat# PHG0311; GIBCO), 10 ng/ml human recombinant basic fibroblast growth factor (bFGF; cat# PHG0266; GIBCO), 100 IU/ml penicillin, 100 μg/ml streptomycin, 2% B27 supplement (cat# 17504-044; GIBCO), 1% N-2 supplement (cat# 17502-048; GIBCO), and 1% methyl cellulose (cat# M0262; Sigma-Aldrich, St. Louis, MO, USA) to prevent cell aggregation. Cells were subsequently seeded in ultra-low adherence 24-well plates (Corning, NY, USA; 200 viable cells per well) at a density of 10^4 cells/ml. Spheres containing over 100 cells were counted.

Quantitative RT-PCR

Total RNA was isolated from cancer cells according to the standard TRIzol (Takara, Tokyo, Japan) method. cDNA synthesis was performed using PrimeScript RT Master Mix (Takara) according to the manufacturer's instructions. Quantitative PCR was performed with SYBR Premix Ex Taq (cat# DRR081A; Takara) using an ABI StepOne Real-time Detection System. PCR reaction conditions for all assays were 94°C for 30 s followed by 40 cycles of 94°C for 5 s, 60°C for 30 s, and 72°C for 30 s. β-actin mRNA was used as an internal control. RT-PCR primers are presented in Table S3.

Invasion assay

Cell invasion was detected using Transwell chambers (8-μm pore size; Millipore, Billerica, MA, USA) with a Matrigel (BD Biosciences, San Jose, CA, USA) matrix. In brief, 3×10^4 cells were seeded on the upper chamber with serum-free DMEM. DMEM medium with 10% FBS was added to the lower chamber. After 24 h, HCC cells that invaded through the Matrigel-coated Transwell inserts were fixed in 95% ethanol and stained with a 4 g/l crystal violet solution. Photographs of three randomly selected fields of fixed cells were captured, and cells were counted. Each experiment was repeated three times.

Colony formation assay

Cells were seeded at a density of 3,000 cells per well in 6-well plates and allowed to grow for 10 days. Next, the colonies were fixed in 4% methanol and stained with a 4 g/l crystal violet solution. Colonies containing over 50 cells were counted.

Collection of CM

CAFs or HCC cells were seeded on 6-well plates at 1×10^5 cells per well. Culture medium was removed 72 h after cell seeding. Cells were washed twice with PBS, and 1 ml of serum-free medium was added per well. After 24 h of incubation at 37°C and 5% CO_2 atmosphere, the CM was collected and passed through a 0.2-mm membrane syringe filter to remove any cells and cell debris.

Human cytokine antibody array

The profiles of cytokine secreted by CAFs and MHCC-97H were detected with the culture supernatants of CAFs and MHCC-97H using a Human cytokine Array (RayBiotech AAH-CYT-5, Norcross, GA) according to the manufacturer's instructions. The cytokines with significant differences in expression were screened out.

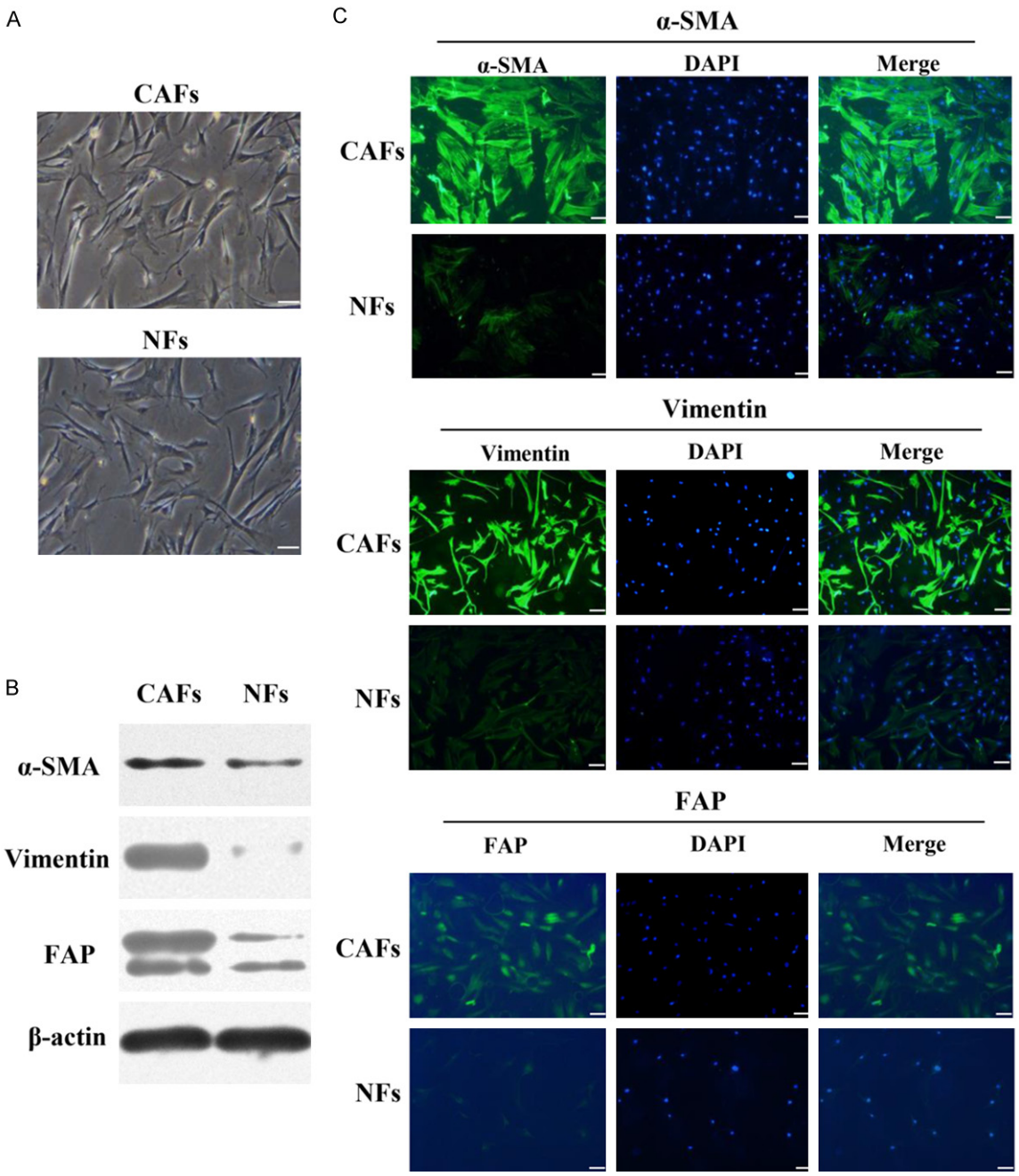

Figure S1. Characteristics of CAFs isolated from HCC patients. (A) Representative morphologies of CAFs and PTFs derived from HCC patients. Scale bar, 100 μm. (B and C) Expression levels of α-SMA, FAP, and vimentin in isolated fibroblasts were determined by western blot (B) and immunofluorescent staining (C). Scale bar, 100 μm. CAFs expressed higher levels of α-SMA, FAP, and vimentin than PTFs.

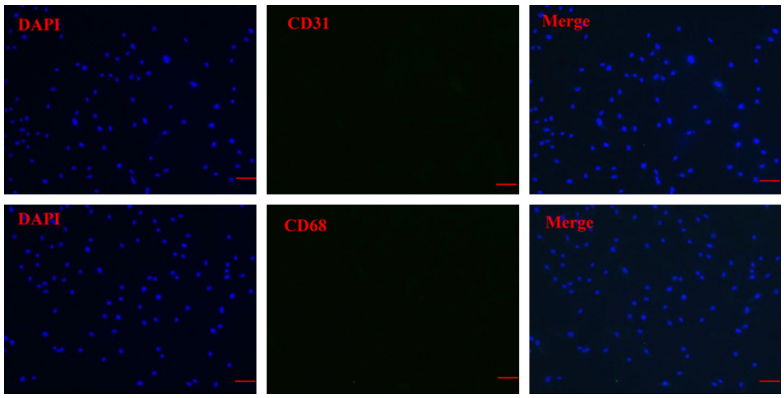

Figure S2. As assessed by immunofluorescent staining, the established CAFs showed negative expression for the endothelial marker CD31 and macrophage markers CD68. Scale bar, 100 μm.

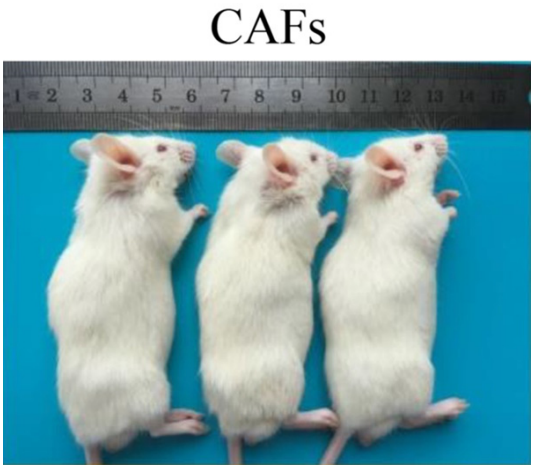

Figure S3. Detection of tumorigenesis of CAFs. CAFs (4×10^5) were injected into nude mice subcutaneously, and no tumors were detected in the mice after 35 days.

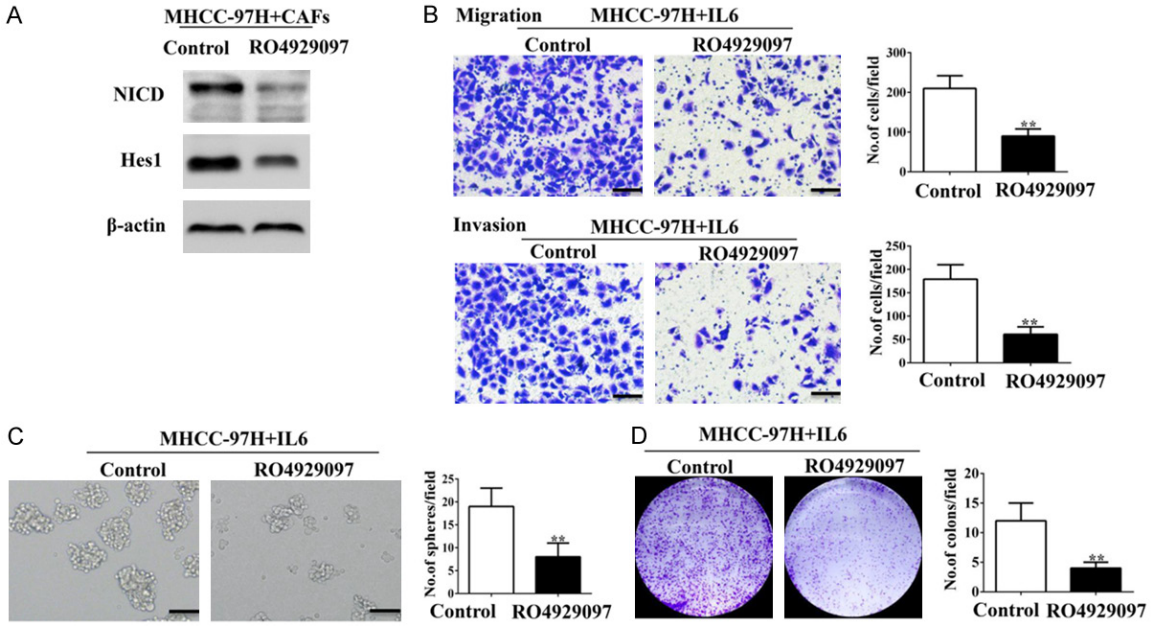

Figure S4. RO4929097 inhibited the CAFs-induced promotion of stem cell-like properties in HCC cells. RO4929097 suppressed the expression of Notch signaling-associated components (NICD, and Hes1) in MHCC-97H cells co-cultured with CAFs. (A) CAFs-induced migration, invasion (B) sphere-forming (C) and colony-forming (D), abilities of MHCC-97H cells decreased when Notch signaling was inhibited by RO4929097. Scale bar, 100μm. Data are shown as means ± SD from at least three independent experiments. (*P < 0.05, **P < 0.01).

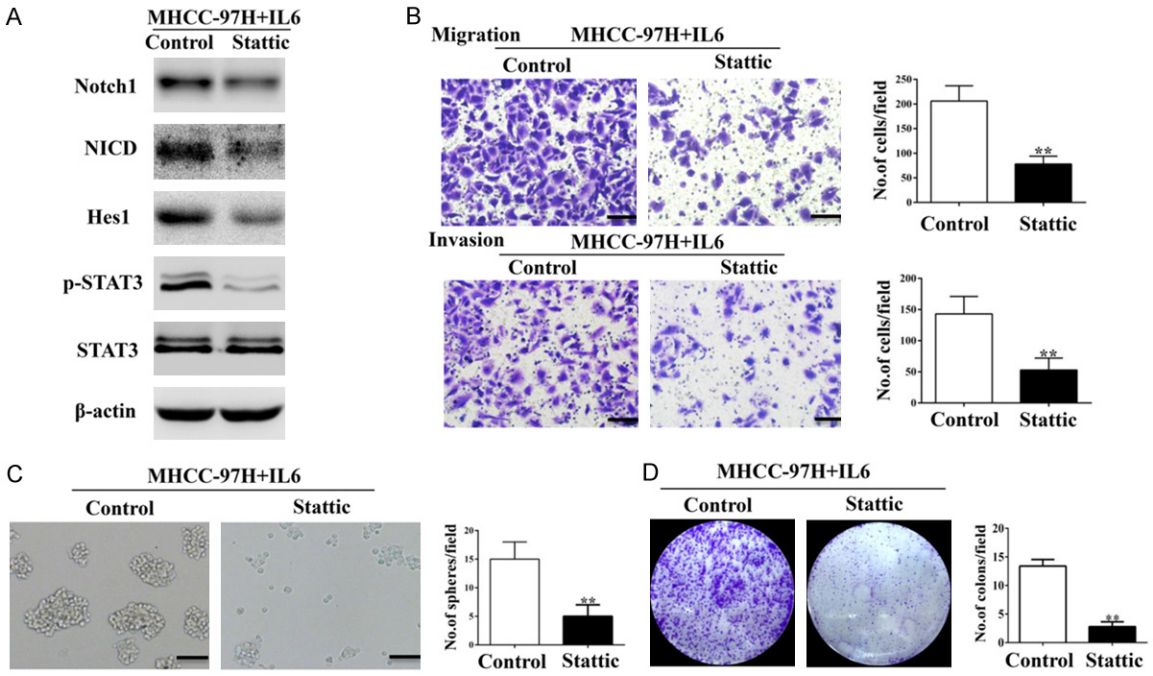

Figure S5. Stattic suppressed the expression of phospho-STAT3 and Notch signaling components (Notch1, NICD, and Hes1) in MHCC-97H cells treated with IL-6. (A) IL-6-induced migration, invasion (B) sphere-forming (C) and colony-forming (D), abilities of MHCC-97H cells decreased when STAT3 Tyr705 phosphorylation was inhibited by Stattic. Scale bar, 100μm. Data are shown as means ± SD from at least three independent experiments. (*P < 0.05, **P < 0.01).

Table S1. The correlation between α-SMA expression and nNICD expression in HCC patients

Variables	High α-SMA N=37	Low α-SMA N=51	*p* Value
Expression of nNICD			
Low	27	46	
High	10	5	P=0.034*

*P < 0.05, Signiicant difference, **P < 0.01, Signiicant difference (χ^2 test and Fisher's exact test).

Table S2. Tumor engraftment rates of HCC cells

Tumor engraftment rates of HCC cells which were injected into the subcutaneous tissue of NOD/SCID mice

Cell type	Cell numbers injected	Tumor incidence	Latency (days)[1]
CAFs	4×10^5	0/3	-
CAFs	2×10^5	0/3	-
CAFs	1×10^5	0/3	-
MHCC-97H cells	1×10^5	3/3	14
MHCC-97H cells	5×10^4	3/3	15
MHCC-97H cells	1×10^4	1/3	18
MHCC-97H cells +CAFs (1:1)	1×10^5	3/3	11
MHCC-97H cells +CAFs (1:1)	5×10^4	3/3	12
MHCC-97H cells +CAFs (1:1)	1×10^4	3/3	15
PLC/PRF/5 cells	1×10^5	2/3	15
PLC/PRF/5 cells	5×10^4	1/3	17
PLC/PRF/5 cells	1×10^4	0/3	-
PLC/PRF/5 cells +CAFs (1:1)	1×10^5	3/3	12
PLC/PRF/5 cells +CAFs (1:1)	5×10^4	3/3	14
PLC/PRF/5 cells +CAFs (1:1)	1×10^4	1/3	21

1, Approximate No. of days from tumor cell injection to the first appearance of tumors.

Tumor engraftment rates of HCC cells which were injected into the liver of NOD/SCID mice

Cell type	Cell numbers injected	Tumor incidence
shCtl-MHCC-97H cells	2×10^5	1/3
shCtl-MHCC-97H cells	1×10^5	0/3
shCtl-MHCC-97H cells	5×10^4	0/3
shCtl-MHCC-97H Cells + CAFs (1:1)	2×10^5	3/3
shCtl-MHCC-97H Cells + CAFs (1:1)	1×10^5	3/3
shCtl-MHCC-97H Cells + CAFs (1:1)	5×10^4	2/3

Cells + CAFs (1:1)		
shCtl-MHCC-97H	2×10^5	3/3
Cells + IL6		
shCtl-MHCC-97H	1×10^5	3/3
Cells + IL6		
shCtl-MHCC-97H	5×10^4	2/3
Cells + IL6		
shNOTCH1-MHCC-97H cells	2×10^5	1/3
shNOTCH1-MHCC-97H cells	1×10^5	0/3
shNOTCH1-MHCC-97H cells	5×10^4	0/3
shNOTCH1-MHCC-97H cells + CAFs (1:1)	2×10^5	3/3
shNOTCH1-MHCC-97H cells + CAFs (1:1)	1×10^5	0/3
shNOTCH1-MHCC-97H cells + CAFs (1:1)	5×10^4	0/3
shNOTCH1-MHCC-97H cells + IL6	2×10^5	1/3
shNOTCH1-MHCC-97H cells + IL6	1×10^5	0/3
shNOTCH1-MHCC-97H cells + IL6	5×10^4	0/3
MHCC-97H cells + IL6	2×10^5	3/3
MHCC-97H cells + IL6	1×10^5	2/3
MHCC-97H cells + IL6	5×10^4	2/3
MHCC-97H cells + IL6 + cryptotanshinone	2×10^5	0/3
MHCC-97H cells + IL6 + cryptotanshinone	1×10^5	0/3
MHCC-97H cells + IL6 + cryptotanshinone	5×10^4	0/3

Table S3. Sequences of primer

Gene	Sequences
Notch1	5’-CCGCAGTTGTGCTCCTGAA-3’
	5’-ACCTTGGCGGTCTCGTAGCT-3’
Hes1	5’-GCTAAGGTGTTTGGAGGCT-3’
	5’-CCGCTGTTGCTGGTGTA-3’
Nanog	5’-GTCCCAAAGGCAAACAACCC-3’
	5’-GCTGGGTGGAAGAGAACACA-3’
Sox2	5’-GCCCTGCAGTACAACTCCAT-3’
	5’-GACTTGACCACCGAACCCAT-3’
Oct4	5’-CTTGAATCCCGAATGGAAAGGG-3’
	5’-GACTTGACCACCGAACCCAT-3’
Fzd7	5’-GTGCCAACGGCCTGATGTA-3’
	5’-AGGTGAGAACGGTAAAGAGCG-3’
Gli1	5’-TGTGGGGACAGAAGTCAAGT-3’
	5’-GCCAATGGAGAGATGACCGT-3’
Smo	5’-CTGTCCTGCGTCATCATCTTT-3’
	5’-CCACAGCAAGGATTGCCAC-3’
β-actin	5’-GTTGCGTTACACCCTTTCTTG-3’
	5’-GACTGCTGTCACCTTCACCGT-3’
c-MYC	5’-GGCTCCTGGCAAAAGGTCA-3’
	5’-CTGCGTAGTTGTGCTGATGT-3’